Article

Metallosupramolecular Polyelectrolytes Self-Assembled from Various Pyridine Ring-Substituted Bisterpyridines and Metal Ions: Photophysical, Electrochemical, and Electrochromic Properties

Fu She Han, Masayoshi Higuchi, and Dirk G. Kurth

J. Am. Chem. Soc., **2008**, 130 (6), 2073-2081 • DOI: 10.1021/ja710380a

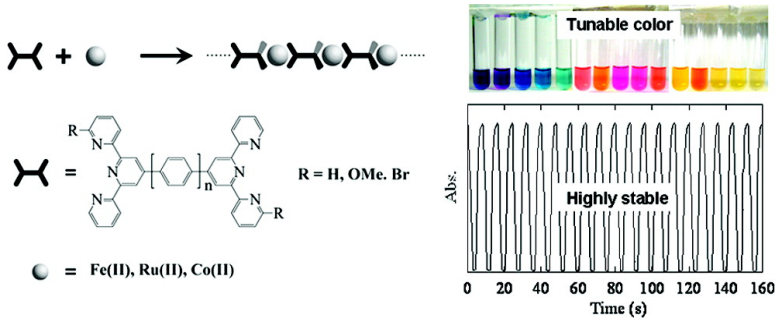

More About This Article

Additional resources and features associated with this article are available within the HTML version:

- Supporting Information
- Links to the 4 articles that cite this article, as of the time of this article download
- Access to high resolution figures
- Links to articles and content related to this article
- Copyright permission to reproduce figures and/or text from this article

View the Full Text HTML

J|A|C|S
ARTICLES
Published on Web 01/18/2008

Metallosupramolecular Polyelectrolytes Self-Assembled from Various Pyridine Ring-Substituted Bisterpyridines and Metal Ions: Photophysical, Electrochemical, and Electrochromic Properties

Fu She Han,[†] Masayoshi Higuchi,*[,†] and Dirk G. Kurth*[,†,‡]

Functional Modules Group, Organic Nanomaterials Center, National Institute for Materials Science, 1-1 Namiki, Tsukuba, Ibaraki 305-0044, Japan, and Max Planck Institute of Colloids and Interfaces, Research Campus Golm, D-14424, Germany

Received November 16, 2007; E-mail: higuchi.masayoshi@nims.go.jp; kurth@mpikg.mpg.de

Abstract: This work presents several metallosupramolecular coordination polyelectrolytes (MEPEs) self-assembled from rigid, π-conjugated, pyridine ring functionalized bisterpyridines and metal ions. The MEPEs are water-soluble and display different colors spanning the entire visible regions. Optical, electrochemical, and electrochromic properties of the obtained MEPEs are presented. The results show that the properties are profoundly affected by the nature of the substituents at the peripheral pyridine rings. Namely, MEPEs assembled from the electron-rich OMe group modified ligands exhibit high switching reversibility and stability and show a lower switching potential than the unsubstituted and electron-deficient Br-substituted analogues. The response times can be tuned either by the design of the ligands or by the choice of the metal ions to cover a broad time scale from under 1 s to several minutes. The optical memory is enhanced from 30 s to longer than 15 min as a comparison of unsubstituted and substituted MEPEs shows. Thus, the significantly enhanced stability and the ease of tuning the properties render this type of supramolecular assembly attractive as electrochromic materials for applications in a large variety of areas. Most importantly, we presented the structure−property relationships of MEPEs, which lays the groundwork for further design of new bisterpyridine-based metallosupramolecular functional materials.

Introduction

Electrochromic materials (ECMs) have received great interest as molecular switches for optical and electronic applications.[1] Commercial applications include a large range of areas, such as anti-glare mirrors and glasses, indicators and labels, smart windows, and information storage, where most applications require electrochromic materials with high contrast ratio, good coloration efficiency, long-term stability, and write-erase efficiency. Some parameters such as response rates and optical memory are application-dependent; for instance, displays need fast switching rates, whereas smart windows can operate with longer response times of up to several minutes. For these purposes, a vast number of materials have been studied,[2] and conducting polymers,[2] molecular dyes,[3] and metal oxides[2,4] are the most frequently investigated components. Generally, conducting polymers show several advantages over molecular dyes and metal oxides, such as the high coloration efficiency, fast switching rates, ease of processing, and the possibility to tune the properties through chemical modification.[5]

Although metal coordination complexes have not been investigated in depth,[6] a few reports associated with polypyridyl[7] and porphyrin[8] complexes indicate that such complexes are potential candidates for the fabrication of ECMs with high performance. Transition-metal complexes are characterized by metal-centered sites with redox-active metal-to-ligand charge transfer (MLCT), intervalence CT, and intraligand transitions, giving rise to strong optical contrast, high coloration ability,

[†] National Institute for Materials Science.
[‡] Max-Planck-Institute.

(1) (a) Monk, P. M. S.; Mortimer, R. J.; Rosseinsky, D. R. *Electrochromism: Fundamentals and Applications*; Wiley-VCH: Weinheim, Germany, 1995. (b) Mortimer, R. J. *Chem. Soc. Rev.* **1997**, *26*, 147.
(2) Mortimer, R. J.; Dyer, A. L.; Reynolds, J. R. *Displays* **2006**, *27*, 2 and references therein.
(3) Sapp, S. A.; Sotzing, G. A.; Reynolds, J. R. *Chem. Mater*. **1998**, *10*, 2101 and references therein.
(4) (a) Granqvist, C. G. *Handbook of Inorganic Electrochromic Materials*; Elsevier: Amsterdam, 1995. (b) Liu, S.; Kurth, D. G.; Möhwald, H.; Volkmer, D. *Adv. Mater.* **2002**, *14*, 225 and references therein.
(5) (a) Kumar, A.; Welsh, D. M.; Morvant, M. C.; Piroux, F.; Abboud, K. A.; Reynolds, J. R. *Chem. Mater.* **1998**, *10*, 896. (b) Gaupp, C. L.; Welsh, D. M.; Reynolds, J. R. *Macromol. Rapid Commun*. **2002**, *23*, 885. (c) Sonmez, G.; Meng, H.; Wudl, F. *Chem. Mater*. **2004**, *16*, 574.
(6) (a) Meyer, T. J. *Acc. Chem. Res*. **1989**, *22*, 163. (b) Balzani, V.; Scandola, F. *Supramolecular Photochemistry*; Ellis Harwood: Chichester, U.K., 1990. (c) Mortimer, R. J.; Rowley, N. M. In *Comprehensive Coordination Chemistry II: From Biology to Nanotechnology*; McCleverty, J. A., Meyer, T. J., Eds.; Elsevier: Oxford, 2004; Vol. 9, pp 581−619. (d) Monk, P. M. S.; Mortimer, R. J.; Rosseinsky, D. R. *Electrochromism and Electrochromic Devices*; Cambridge University Press: Cambridge, 2007; p 253.
(7) (a) *Chem. Eng. News* **1983**, *61*, 21. (b) Leasure, R. M.; Ou, W.; Moss, J. A.; Linton, R. W.; Meyer, T. J. *Chem. Mater*. **1996**, *8*, 264. (c) Pichot, F.; Beck, J. H.; Elliott, C. M. *J. Phys. Chem. A* **1999**, *103*, 6263. (d) Kimura, M.; Horai, T.; Muto, T.; Hanabusa, K.; Shirai, H. *Chem. Lett.* **1999**, 1129. (e) Bernhard, S.; Goldsmith, J. I.; Takada, K.; Abruña, H. D. *Inorg. Chem*. **2003**, *42*, 4389. (f) Kurth, D. G.; López, J. P.; Dong, W. F. *Chem. Commun.* **2005**, 2119.
(8) Trombach, N.; Hild, O.; Schlettwein, D.; Wöhrle, D. *J. Mater. Chem*. **2002**, *12*, 879.

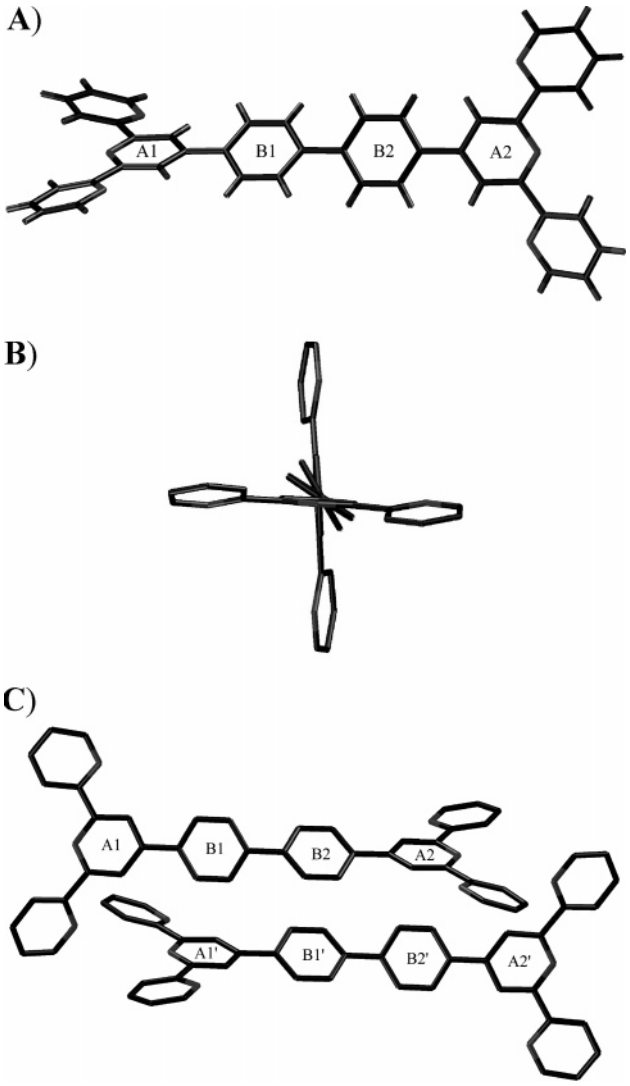

Figure 1. X-ray crystal structure of **L2**. (A) Top view. (B) Side view. (C) Molecular stacking in the crystal lattice. Hydrogen atoms in B and C are omitted for clarity. Crystal data at 110 K: $C_{42}H_{28}N_6$ (MW: 616.71), 0.20 × 0.05 × 0.04 mm^3, colorless crystalline needles, monoclinic space group *C*2/*c*, $a = 28.0200(12)$ Å, $b = 10.6337(3)$ Å, $c = 10.9221(4)$ Å, $V = 3201.6(2)$ Å^3, $\beta = 100.330(3)°$, $Z = 4$; final R1 = 0.0445 for all 15 519 reflections of $I > 2\sigma(I)$, wR2 = 0.1404 for all 15 519 reflections.

and low switching potential.[9] Furthermore, the properties of the complexes can be modified by changing the ligands or metal ions.[10] Finally, processing preferentially from aqueous media in various device configurations such as nanostructures,[11] thin films,[12] mesophases,[13] and liquid crystalline and gel[14] represents an added advantage of using coordination complexes for practical applications as ECMs.

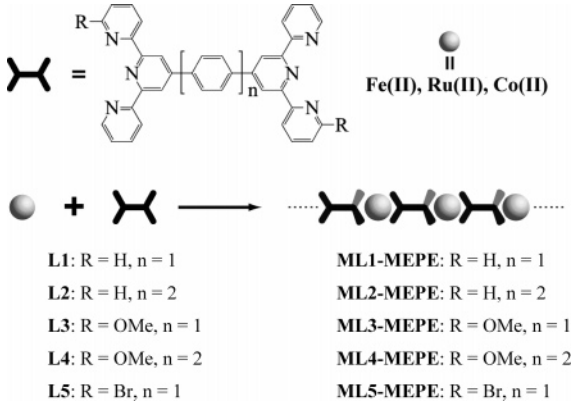

Figure 2. Structures of ligands **L1**−**L5** and the corresponding MEPEs **ML1-MEPE**−**ML5-MEPE**, where **M** indicates the metal ion Fe(II), Ru(II), and Co(II), **L** represents the ligands, and MEPE stands for metallosupramolecular coordination polyelectrolytes.

Thus far, terpyridines, bipyridines, and porphyrins have been investigated,[2] and of the available ligands, terpyridines are particularly interesting. This type of ligand has a rich coordination chemistry and generally displays a high binding affinity to many metal ions,[10] offering the thermodynamic driving force for stable metallosupramolecular formation.[10,15] Furthermore, use of terpyridine ligands affords a well-defined coordination geometry, preventing diastereoisomeric formation as appeared with their sister bipyridines. This is an important issue in particular if multinuclear polymer, which is advantageous for processing, is under consideration.[10a]

During the development of new metallosupramolecule-based ECMs, we paid attention to rigid, π-conjugated bisterpyridines having substituents at the 6-position of the pyridine ring as contrasted with the unsubstituted analogues reported in previous reports.[7c−e] We reasoned that a functional group at the 6-position of the pyridine periphery will influence through steric or electronic effects the ligand field stabilization energy and, thus, the properties of the metallosupramolecular assemblies. On the other hand, to investigate in systematic ways the structure−property relationships, which are virtually unknown but are highly desirable for the design of new functional materials, we focus on the synthesis of a range of different metallosupramolecular coordination polyelectrolytes (MEPEs). Thus, a series of bisterpyridines having electron-rich or -deficient functionalities was synthesized, from which several MEPEs were assembled using Fe(II), Ru(II), and Co(II) as metal ions. Electrochromic studies of the resulting MEPEs reveal that the relevant properties of these materials, such as optical absorption, color, switching potential, response time, stability, reversibility, and optical memory, can be readily tuned either by the proper design of the ligands or by the choice of the metal ions, making this class of metallosupramolecular assemblies highly attractive for electrochromic applications.

Results and Discussion

Synthesis of Ligands and Metallosupramolecular Polymers. L1 (Figure 2) is commercially available. Ligands **L2** and

(9) (a) Roundhill, D. M. *Photochemistry and Photophysics of Metal Complexes*; Plenum Press: New York, 1994. (b) Juris, A.; Balzani, V.; Barigelletti, F.; Campagana, S.; Belser, P.; Von Zelewsky, A. *Coord. Chem. Rev.* **1988**, *84*, 85.
(10) For reviews, see: (a) Constable, E. C. *Chem. Soc. Rev.* **2007**, *36*, 246. (b) Kurth, D. G.; Higuchi, M. *Soft Matter* **2006**, *2*, 915. (c) Andres, P. R.; Schubert, U. S. *Adv. Mater.* **2004**, *16*, 1043.
(11) (a) Kurth, D. G.; Lehmann, P.; Schütte, M. *Proc. Natl. Acad. Sci. U.S.A.* **2000**, *97*, 5704. (b) Kurth, D. G.; Severin, N.; Rabe, J. P. *Angew. Chem., Int. Ed.* **2002**, *41*, 3681; *Angew. Chem.* **2002**, *114*, 3833.
(12) (a) Schütte, M.; Kurth, D. G.; Linford, M. R.; Cölfen, H.; Möhwald, H. *Angew. Chem., Int. Ed.* **1998**, *37*, 2891; *Angew. Chem.* **1998**, *110*, 3058. (b) Lehmann, P.; Kurth, D. G.; Brezesinski, G.; Symietz, C. *Chem.—Eur. J.* **2001**, *7*, 1646.
(13) Kurth, D. G.; Meister, A.; Thunemann, A. F.; Forster, G. *Langmuir* **2003**, *19*, 4055.
(14) (a) Aamer, K. A.; Tew, G. N. *Macromolecules* **2007**, *40*, 2737. (b) Camerel, F.; Ziessel, R.; Donnio, B.; Bourgogne, C.; Guillon, D.; Schmutz, M.; Iacovita, C.; Bucher, J. P. *Angew. Chem., Int. Ed.* **2007**, *46*, 2659.
(15) (a) Iyer, P. K.; Beck, J. B.; Weder, C.; Rowan, S. J. *Chem. Commun.* **2005**, 319. (b) Yount, W. C.; Juwarker, H.; Craig, S. L. *J. Am. Chem. Soc.* **2003**, *125*, 15302.

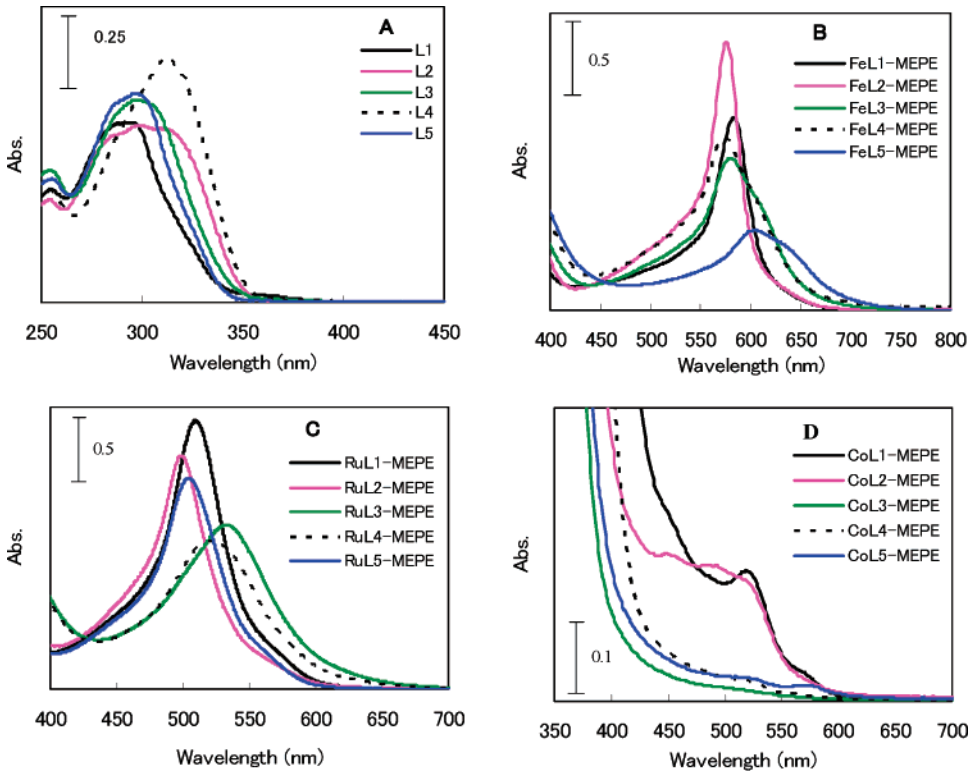

Figure 3. UV−vis spectra of free ligands **L1**−**L5** in 10 μM CH_2Cl_2 solution (A), **FeL1-MEPE**−**FeL5-MEPE** in 70 μM MeOH solution (B), **RuL1-MEPE**−**RuL5-MEPE** in 50 μM MeOH/H_2O (v/v = 4:1) solution (C), and **CoL1-MEPE**−**CoL5-MEPE** in 70 μM MeOH solution (D).

L4 were synthesized according to a one-pot Suzuki-type dimerization[16] as shown in Scheme S1. Syntheses of ligands **L3** and **L5** were carried out employing a two-step Kröhnke approach[17] (Scheme S2). X-ray analysis[18] of **L2** indicates that this ligand takes a straight rigid conformation along the central axis of ring A1−B1−B2−A2 (Figure 1A). The dihedral angles between the rings A1 and B1, B1 and B2, and A1 and A2 are 27.976 (6)°, 27.302 (3)°, and 83.243 (2)°, respectively. A side view reveals that the two terpyridine planes are almost perpendicular with a calculated dihedral angle of 83.243 (2)° between rings A1 and A2 (Figure 1B). In the crystal lattice, the molecules displace from each other by about 4.33 Å along the A1−B1−B2−A2 central axis, a distance approximately corresponding to the length of a C−C bond and the diagonal distance of a benzene ring (Figure 1C). The dihedral angles between the rings B1 and A1′, B2 and B1′, and A2 and B2′ are calculated to be 55.269 (3)°, 0°, and 55.269 (3)°, respectively. The calculated centroid-to-centroid distances between the rings B1 and A1′, B2 and B1′, and A2 and B2′ are 4.451(1), 4.345-(1), and 4.442 Å, respectively, indicating only weak interlayer $\pi-\pi$ interaction. Owing to the rigid structure and linear connectivity of the metal ion receptor, it is anticipated that well-defined rodlike MEPEs are formed from **L2** and its analogue ligands, **L1**[19] (Figure 2) and **L3**−**L5**, avoiding ring formation as detected with less rigid ligands.[20]

Coordination polymerization of various MEPEs was performed by heating an equimolar amount of ligand and metal ion in a suitable solvent (Figure 2). While self-assembly with kinetically labile metal ions such as Fe(II) or Co(II) occurs at room temperature even in water, refluxing in solvent significantly accelerates product formation. The Co(II)-based MEPEs, **CoL1-MEPE**−**CoL5-MEPE**, were assembled by refluxing ligands and $Co(OAc)_2$ in MeOH. The Ru(II)-based MEPEs, **RuL1-MEPE**−**RuL5-MEPE**, were prepared by stirring a mixture of ligands and $RuCl_2(DMSO)_4$ in ethylene glycol at 150 °C. The Fe(II)-based MEPEs, **FeL1-MEPE**−**FeL5-MEPE**, were prepared according to the previously published procedure.[21] All MEPEs exhibit moderate to good solubility in H_2O, MeOH, EtOH, and HOAc, and some of them are also soluble in THF and $CHCl_3$, making these materials processable from various solvent systems, including environmentally friendly aqueous media. As a comparison, the solubilities of their PF_6^- and ClO_4^- forms are much poorer. The formation of coordination complexes was confirmed by using UV−vis spectroscopy and ESI-TOF high-resolution mass analysis.

Optical Properties. The optical properties of the ligands **L1**−**L5** and their corresponding Fe(II)-, Ru(II)-, and Co(II)-MEPEs are investigated by UV−vis spectroscopy. The spectra are shown in Figure 3, and the spectroscopic data are collected in Table 1. For comparison, the absorption data of Fe(II)-based MEPEs published previously is also included.[21] For the five ligands (Figure 3A and Table 1), an increase in the spacer length from one phenylene to two phenylene units and the introduction of either electron-donating OMe, **L3** and **L4**, or electron-withdrawing Br groups, **L5**, result in a slight shift of the $\pi-\pi^*$ transition bands toward longer wavelength, giving rise to a red shift of

(16) Han, F. S.; Higuchi, M.; Kurth, D. G. *Org. Lett.* **2007**, *9*, 559.
(17) Eryazici, I.; Moorefield, C. N.; Durmus, S.; Newkome, G. R. *J. Org. Chem.* **2006**, *71*, 1009 and references therein.
(18) See also the Supporting Information of ref 16 for the CIF file of **L2**.
(19) Kolb, U.; Buscher, K.; Helm, C. A.; Lindner, A.; Thunemann, A. F.; Menzel, M.; Higuchi, M.; Kurth, D. G. *Proc. Natl. Acad. Sci. U.S.A.* **2006**, *103*, 10202.
(20) El-Ghayoury, A.; Schenning, A. P. H. J.; Meijer, E. W. *J. Polym. Sci., Part A: Polym. Chem.* **2002**, *40*, 4020.
(21) Han, F. S.; Higuchi, M.; Kurth, D. G. *Adv. Mater.* **2007**, *19*, 3928.

Table 1. UV−Vis Properties of Free Ligands **L1**−**L5** and Their Corresponding Fe(II)-, Ru(II)-, and Co(II)-Based MEPEs[a]

entries	λ_{max} (nm)[b] (ϵ [M^{-1} cm^{-1}])	entries	λ_{max} (nm)[b] (ϵ [M^{-1} cm^{-1}])
L1	292[c] (61 300)	**RuL1-MEPE**	513 (40 960)
L2	310 (59 800)	**RuL2-MEPE**	502 (35 520)
L3	298 (68 500)	**RuL3-MEPE**	536 (25 420)
L4	316 (81 400)	**RuL4-MEPE**	524 (22 520)
L5	299 (70 600)	**RuL5-MEPE**	507 (32 460)
FeL1-MEPE[d]	586 (18500)	**CoL1-MEPE**	522 (2514)
FeL2-MEPE	579 (25700)	**CoL2-MEPE**	521 (2300)
FeL3-MEPE	585 (616) (14300)	**CoL3-MEPE**	521 (214)
FeL4-MEPE	578 (614) (16700)	**CoL4-MEPE**	519 (457)
FeL5-MEPE	612 (639) (7700)	**CoL5-MEPE**	526 (429)

[a] At room temperature, in CH_2Cl_2 (10 μM) for ligands **L1**−**L5**; in MeOH (70 μM) for **FeL1-MEPE**−**FeL5-MEPE**; in MeOH/H_2O (4/1, 50 μM) for **RuL1-MEPE**−**RuL5-MEPE**; and in MeOH (70 μM) for **CoL1-MEPE**−**CoL5-MEPE**. [b] The maximum absorption (λ_{max}) and molar absorptivity (ϵ_{max}) are given as $\pi-\pi^*$ transition for ligands **L1**−**L5**; MLCT for **FeL1-MEPE**−**FeL5-MEPE** and **RuL1-MEPE**−**RuL5-MEPE**; and $d-d^*$ transition for **CoL1-MEPE**−**CoL5-MEPE**. [c] See also ref 22 for absorption data of ligands **L1** and **L2**. [d] Data for Fe(II)-based MEPEs taken from ref 21.

up to 15 nm when **L4** and **L1** are compared. On the other hand, the absorption intensity remains unchanged by varying the spacer length from one to two phenylene units;[22] however, incorporation of OMe or Br substituents at the 6-position of the pyridine ring results in an increased absorbance (**L3**−**L5**).

A profound influence of the ligands on the optical properties of the corresponding metallosupramolecular assemblies is observed. Panels B and C of Figure 3 depict the UV−vis spectra of Fe(II)- and Ru(II)-MEPEs, respectively, and the spectroscopic data are listed in Table 1. For the Fe(II)-MEPEs, a strong absorption band occurs around 580 nm, which is characteristic of MLCT of the bisterpyridine−Fe(II) complex with a quasi-octahedral coordination geometry.[23] For the Ru(II)-MEPEs, a strong band around 520 nm is present, which can be assigned to the MLCT of complexes between terpyridine and Ru(II).[24] Similar to the Fe(II)-based polymers, the MLCT bands of Ru(II)-MEPEs are blue-shifted by approximately 10 nm when the spacer length is increase from one to two phenylene groups (**RuL1-MEPE** vs **RuL2-MEPE**), and the introduction of electron-rich OMe or -deficient Br groups at the pyridine periphery leads to a smaller ϵ_{max} as a comparison of **RuL3-MEPE**−**RuL5-MEPE** vs unsubstituted **RuL1-MEPE** and **RuL2-MEPE** shows. However, somewhat different from the behavior exhibited by the Fe(II)-MEPEs, electron-rich OMe groups cause a large red shift of the MLCT of more than 20 nm in the Ru(II)-MEPEs as a comparison of **RuL3-MEPE** vs **RuL1-MEPE** and **RuL4-MEPE** vs **RuL2-MEPE** shows, whereas electron-deficient Br groups slightly blue shift (ca. 6 nm) the MLCT band when **RuL5-MEPE** and **RuL1-MEPE** are compared. In addition, an increase in the spacer length results in a smaller ϵ_{max} value (**RuL1-MEPE** vs **RuL2-MEPE** and **RuL3-MEPE** vs **RuL4-MEPE**). These behaviors are reversed when Fe(II) instead of Ru(II) is used as metal ion.[21] Depending on the metal ion, the increase in spacer length of the ligand associated with an increased or a decreased ϵ_{max} is also observed for the mono- or dinuclear complexes prepared from **L1** and **L2**.[22,24] Finally, it should be mentioned that as an important parameter for electrochromic application, ϵ_{max} of the MLCT bands of Ru(II)-based MEPEs is generally much higher than that of the corresponding Fe(II)-based analogues.

Figure 3D shows the UV−vis spectra of Co(II)-MEPEs; the spectroscopic data are listed in Table 1. No MLCT is observed for this series; instead, a weak $d-d^*$ transition band of Co(II) around 520 nm appears for all five polymers.[7f] Similar to that of the two series of MEPEs based on Fe(II) and Ru(II) ions, the ligand-dependent changes in $d-d^*$ transitions of Co(II)-MEPEs clearly show that ϵ_{max} is reduced largely by attaching either electron-donating OMe groups or -withdrawing Br groups, although only a weak effect on λ_{max} is observed.

The significant effect of the ligand structure and the metal ion on the optical properties of the resulting assemblies is easily recognized by the different colors displayed by MEPEs. Accordingly, the Fe(II)-MEPEs **FeL1-MEPE**−**FeL5-MEPE** are dark-blue, purple, blue, sky-blue, and grass-green, respectively (Figure 4A). The Ru(II)-MEPEs **RuL1-MEPE**−**RuL5-MEPE** show magenta, deep-orange, purple-red, violet, and red, respectively (Figure 4B). The Co(II)-MEPEs **CoL1-MEPE**−**CoL5-MEPE** are orange, red, yellow, and pale-yellow, respectively (Figure 4C). Intermediate colors can be realized by mixing different MEPEs in appropriate ratios. Tailoring the color of electrochromic materials remains a particularly important challenge. We show here that the color of bisterpyridine-based coordination polymers is readily tuned to span the entire visible region either by the design of the ligand or by the choice of the metal ion.

Electrochemical Properties. The electrochemical properties of ligands **L1**−**L5** and their corresponding metallosupramolecular assemblies are investigated by cyclic voltammetry or differential pulse voltammetry (DPV). No redox peaks are observed for free ligands. The cyclic voltammograms and the redox potentials ($E_{1/2}$) of the MEPEs are summarized in Figure 5 and Table 2, respectively. The Fe(II)-MEPEs (Figure 5A and Table 2) exhibit a reversible redox potential of the Fe(II)/Fe(III) couple (the potential for **FeL5-MEPE** was determined by DPV). **FeL3-MEPE** and **FeL4-MEPE**, whose ligands are modified by electron-donating OMe groups, display a redox potential at ca. 0.70 V, about 70 mV more negative than the unsubstituted MEPEs **FeL1-MEPE** and **FeL2-MEPE**. In contrast, **FeL5-MEPE**, whose ligand is modified by electron-withdrawing Br groups, shows a potential at ca. 0.93 V, about 160 mV more positive than its unsubstituted analogue **FeL1-MEPE**. However, no significant effect is observed by varying the spacer, as a comparison of **FeL1-MEPE** vs **FeL2-MEPE** and **FeL3-MEPE** vs **FeL4-MEPE** shows.

A similar effect of ligand on the electrochemical property is observed for the MEPEs based on Ru(II) (Figure 5B and Table 2; the voltammogram of **RuL1-MEPE** is not shown for clarity). The OMe group functionalized **RuL3-MEPE** and **RuL4-MEPE**

(22) Auffrant, A.; Barbieri, A.; Barigelletti, F.; Collin, J. P.; Flamigni, L.; Sabatini, C.; Sauvage, J. P. *Inorg. Chem.* **2006**, *45*, 10990.
(23) Sénéchal-David, K.; Leonard, J. P.; Plush, S. E.; Gunnlaugsson, T. *Org. Lett.* **2006**, *8*, 2727.
(24) Haga, M.; Takasugi, T.; Tomie, A.; Ishizuya, M.; Yamada, T.; Hossain, M. D.; Inoue, M. *Dalton Trans.* **2003**, 2069 and references therein.

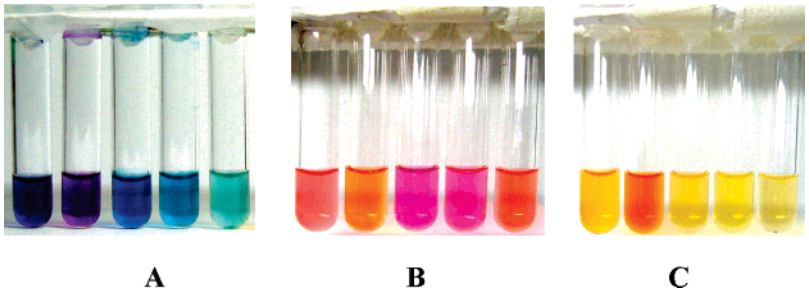

Figure 4. Colors of **FeL1-MEPE**−**FeL5-MEPE** (0.25 mM, MeOH) (A), **RuL1-MEPE**−**RuL5-MEPE** (0.05 mM, MeOH/H_2O (v/v = 4/1)) (B), and **CoL1-MEPE**−**CoL5-MEPE** (0.5 mM, MeOH) (C). Photo of Fe(II)-MEPEs taken from ref 21.

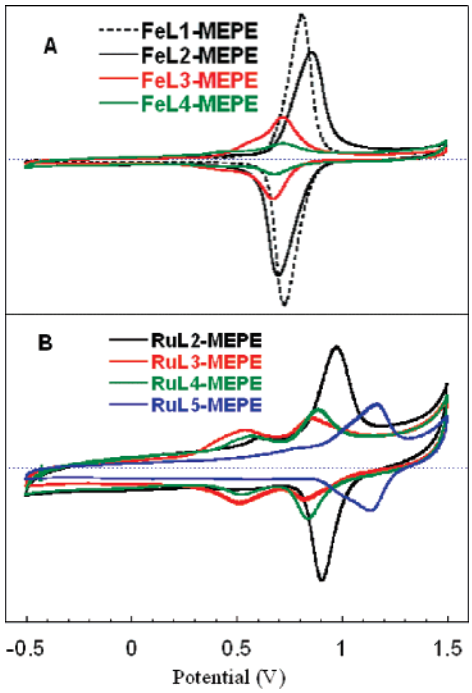

Figure 5. Cyclic voltammograms of Fe(II)- (A) and Ru(II)-MEPEs (B) recorded from thin films coated on a glassy carbon electrode in an electrolyte solution of *n*-Bu_4NClO_4 (0.10 M) in argon-saturated acetonitrile using a platinum wire as counter electrode, and Ag/AgCl electrode as referenced electrode at room temperature with a scan rate of 100 mV s^{-1}.

Table 2. Electrochemical Properties of Fe(II)-, Ru(II)-, and Co(II)-MEPEs[a]

MEPEs	$E_{1/2}$ (V)	MEPEs	$E_{1/2}$ (V)	MEPEs	$E_{1/2}$ (V)
FeL1-MEPE[b]	0.77	**RuL1-MEPE**	0.95	**CoL1-MEPE**	0.02
FeL2-MEPE	0.78	**RuL2-MEPE**	0.95	**CoL2-MEPE**	0.04[c]
FeL3-MEPE	0.70	**RuL3-MEPE**	0.84	**CoL3-MEPE**	*d*
FeL4-MEPE	0.70	**RuL4-MEPE**	0.85	**CoL4-MEPE**	
FeL5-MEPE	0.93	**RuL5-MEPE**	1.16	**CoL5-MEPE**	

[a] Cyclic voltammograms recorded from thin films coated on a glassy carbon electrode in an electrolyte solution of *n*-Bu_4NClO_4 (0.10 M) using a platinum wire as counter electrode, and Ag/AgCl electrode as referenced electrode in argon-saturated acetonitrile at room temperature, with a scan rate of 100 mV s^{-1}. [b] Data for Fe(II)-based MEPEs taken from ref 21. [c] Measured by DPV. [d] Cannot be determined.

display a redox potential at ca. 0.85 V, about 100 mV lower than the unsubstituted MEPEs **RuL1-MEPE** and **RuL2-MEPE** (ca. 0.95 V), respectively. In contrast, the Br group functionalized **RuL5-MEPE** shows a redox potential about 1.16 V, about 210 mV higher than that of unsubstituted **RuL1-MEPE**. The length of spacer does not show an effect on the redox potential. It is thus evident that the electron-donating or -withdrawing nature of the substituents at the peripheral pyridines affects markedly the redox behavior of the MEPEs.[25] In general, the electron-donating group leads to a smaller redox potential while the electron-withdrawing substituent results in a higher one as compared to the unsubstituted analogues. Substitution effect at the spacer region (4′-position of terpyridine) has been extensively studied.[24,26−30]

Of interest is that both the Fe(II) and Ru(II)-MEPEs assembled from the OMe- or Br-substituted ligands, **FeL3-MEPE**−**FeL5-MEPE** and **RuL3-MEPE**−**RuL5-MEPE**, show an additional weak reversible redox waves at a lower potential (see zoomed cyclic voltammograms of the Fe(II)-based MEPEs in Figure S1 for a clear view), while the corresponding unsubstituted MEPEs show only a single wave. The reason is not clear, although extensive control experiments have been performed for clarification. Apparently, the substitution at the 6-position of the pyridine rings with OMe or Br group in ligands **L3**−**L5** is expected to perturb the bond distance and coordination geometry through the electronic and steric effects in particular if the unsymmetric structures of substitution pattern are compared to the symmetrical, unsubstituted ligands **L1** and **L2**. For instance, substitution at this position may affect the equilibrium of high- and low-spin Fe(II) species in MEPE depending on the nature of substitutents,[25] thus presenting two redox waves corresponding to each species. Substitution effect has also been observed in the optical properties of these MEPEs (vide supra).[21]

Investigating the redox behavior of Co(II)-based MEPEs reveals weak redox peaks of the Co(II)/Co(III) couple at 0.02 and 0.04 V for **CoL1-MEPE** and **CoL2-MEPE**, respectively (Table 2), while redox peaks for OMe- and Br-modified analogues **CoL3-MEPE**−**CoL5-MEPE** are not observed.

Electrochromic Properties. The electrochromic nature of MEPEs is examined by probing their reversibility, switching potential, long-term stability, response time, and optical memory.

(25) Constable, E. C.; Baum, G.; Bill, E.; Dyson, R.; Eldik, R.; van Fenske, D.; Kaderli, S.; Morris, D.; Neubrand A.; Neuburger, M.; Smith, D. R.; Wieghardt, K.; Zehnder, M.; Zuberbühler, A. D. *Chem.—Eur. J.* **1999**, *5*, 498.
(26) Fang, Y.; Taylor, N. J.; Laverdière, F.; Hanan, G. S.; Loiseau, F.; Nastasi, F.; Campagna, S.; Nierengarten, H.; Leize-Wagner, E.; Dorsselaer, A. V. *Inorg. Chem.* **2007**, *46*, 2854.
(27) Lainé, P. P.; Bedioui, F.; Loiseau, F.; Chiorboli, C.; Campagna, S. *J. Am. Chem. Soc.* **2006**, *128*, 7510.
(28) Carlson, C. N.; Kuehl, C. J.; Da Re, R. E.; Veauthier, J. M.; Schelter, E. J.; Milligan, A. E.; Scott, B. L.; Bauer, E. D.; Thompson, J. D.; Morris, D. E.; John, K. D. *J. Am. Chem. Soc.* **2006**, *128*, 7230.
(29) Flamigni, L.; Baranoff, E.; Collin, J. P.; Sauvage, J. P. *Chem.—Eur. J.* **2006**, *12*, 6592.
(30) Vaduvescu, S.; Potvin, P. *Eur. J. Inorg. Chem.* **2004**, 1763.

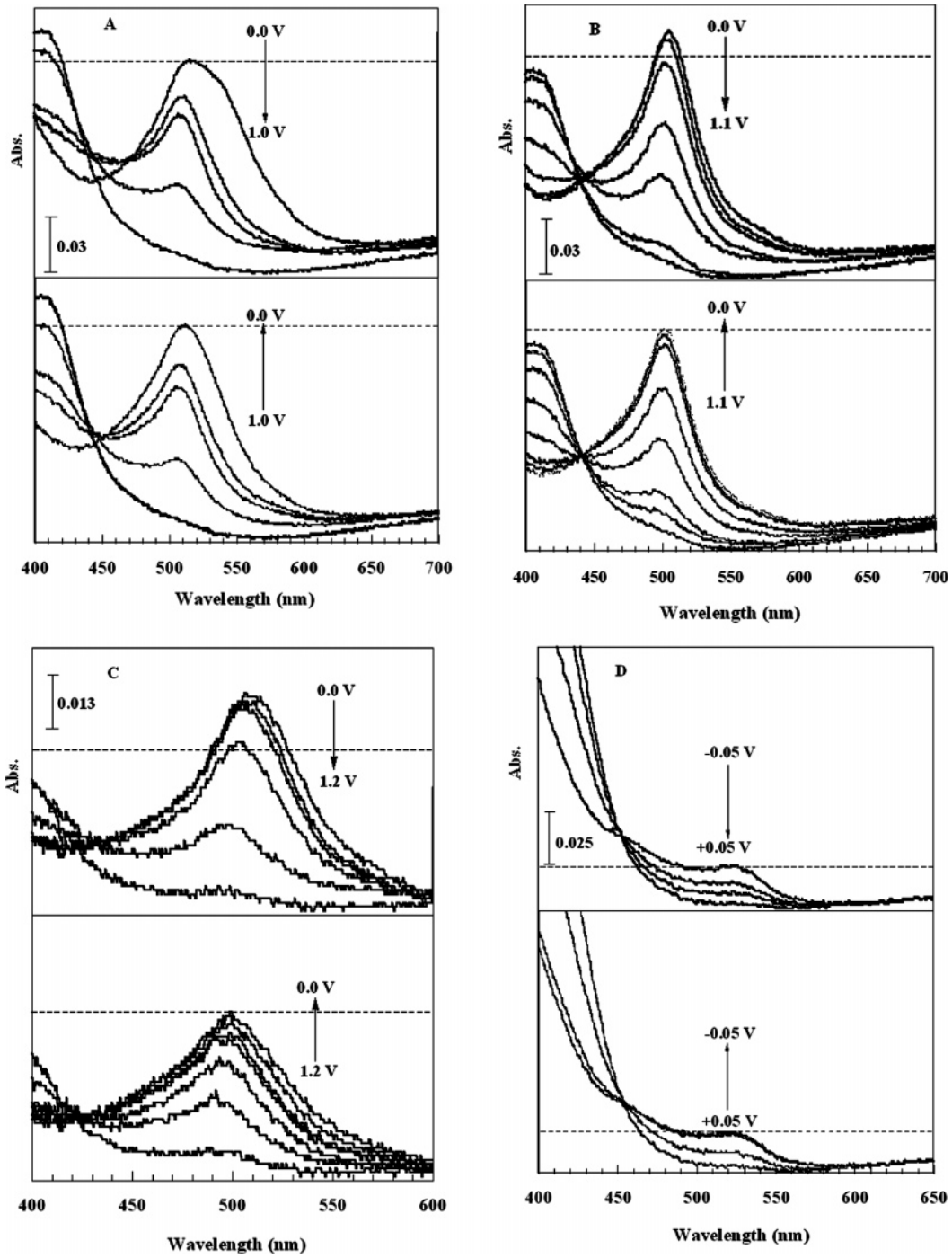

Figure 6. Absorbance changes of **RuL4-MEPE** (A), **RuL2-MEPE** (B), **RuL5-MEPE** (C), and **CoL2-MEPE** (D) films coated on an ITO electrode as representative examples at different potentials (vs Ag/AgCl) in an argon-saturated acetonitrile solution of *n*-Bu_4NClO_4 (0.1 M).

These parameters are important when practical application of an ECM is concerned, but the available ECMs based on metal coordination complexes have not been investigated sufficiently.[7,24]

Switching Reversibility and Potential. To examine the reversibility, the spectral changes of coated ITO slides are recorded as a function of the applied potential. We observed that, for Fe(II)- and Ru(II)-MEPEs, the MLCT absorbance decreases gradually upon incrementally increasing the potential and finally is lost completely to leave the film colorless. However, the recovery of the MLCT band is affected by the nature of the substituents in the peripheral pyridines of the ligands. As examples, the MLCT band of Ru(II)-MEPEs having electron-rich OMe groups recovers completely upon reversing the potential (Figure 6A). The unsubstituted analogues **RuL1-MEPE** and **RuL2-MEPE** (Figure 6B) show a slight loss of their absorbance, although the unsubstituted Fe(II)-MEPEs, **FeL1-MEPE** and **FeL2-MEPE**, exhibit equally good reversibility as the OMe-modified MEPEs, **FeL3-MEPE** and **FeL4-MEPE**. The loss becomes noticeable for **FeL5-MEPE** and **RuL5-MEPE**, whose ligands are modified by electron-deficient Br groups (Figure 6C). The data also reveal that the switching potential of the MEPEs are structure-dependent, which is reduced by introducing OMe groups, but is increased by

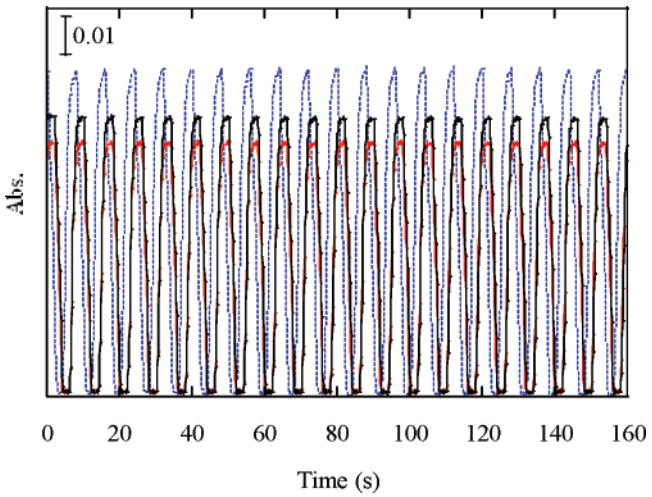

Figure 7. MLCT absorbance change of a thin film of **RuL4-MEPE** at potentials of +1.5 and 0.0 V vs Ag/AgCl with a 4 s delay between switching. First 40 (blue), middle 40 (black), and last 40 (red) of 4000 redox cycles are shown.

appending Br groups, with a scale of 100 mV at least as compared to the unsubstituted polymers.

Finally, the reversibility of Co(II)-MEPEs was probed by inspecting the spectral change of $d-d^*$ transition as a function of the applied potential. Although the spectral changes of the pyridine ring functionalized MEPEs, **CoL3-MEPE**−**CoL5-MEPE**, are difficult to monitor because of the weak absorbance, their unsubstituted analogues, **CoL1-MEPE** and **CoL2-MEPE**, operate reversibly at the applied potentials between −0.5 to +0.5 V, as shown by bleaching and coloration behavior of **CoL2-MEPE** (Figure 6D).

Long-Term Stability. The stability of the bleached and/or colored states toward multiple redox steps represents one of the most important parameters for the practical utilization of ECMs. To inspect the structure-related stability of the obtained supramolecular polymer materials here, we performed a long-term redox switching study by continuously stepping the voltages between two given values, while the optical changes of coated ITO electrodes were monitored as a function of time up to 4000 double-potential cycles.

Figure 7 depicts the results of **RuL4-MEPE** as a representative example over 4000 switching cycles (first 40 (blue), middle 40 (black), and last 40 (red) of 4000 redox cycles are shown). The % loss of the optical intensity of this and the other MEPEs is listed in Table 3. The results suggest that the stabilities are correlated mainly with the structure of the ligands, although an effect of metal ions can also be recognized. We observe a ca. 20% loss of the MLCT intensity for Fe(II)- and Ru(II)-MEPEs assembled from the electron-donating OMe-modified ligands after 4000 cycles (**FeL3-MEPE**, **FeL4-MEPE**, **RuL3-MEPE**, and **RuL4-MEPE**). Interestingly, the main part of the loss is observed in the first several hundreds of redox cycles, after which the absorbance of the device stabilizes. As illustrated with **RuL4-MEPE** (Figure 7), about 12% loss in absorbance intensity is observed in the first 1000 cycles whereas only ca. 10% loss is detected in the following 3000 cycles (ca. 4, 3, and 3% in each thousand of cycles, respectively). After 4000 cycles, the UV−vis spectra of the films are essentially identical to those of original materials in solution (Figure S2). Thus, the loss in absorbance is most likely the desorption of the materials in the solution of supporting electrolyte rather than the redox-induced deterioration or dissociation.

Table 3. Optical Intensity Loss of Various MEPEs after Multiple Steps of Redox Cycles[a]

MEPEs	loss (%)	MEPEs	loss (%)	MEPEs	loss (%)
FeL1-MEPE	21	**RuL1-MEPE**	29	**CoL1-MEPE**	<2[e]
FeL2-MEPE	18	**RuL2-MEPE**	41[c]	**CoL2-MEPE**	<2[e]
FeL3-MEPE	22	**RuL3-MEPE**	19	**CoL3-MEPE**	*f*
FeL4-MEPE	17	**RuL4-MEPE**	22	**CoL4-MEPE**	
FeL5-MEPE	48[b]	**RuL5-MEPE**	49[d]	**CoL5-MEPE**	

[a] Unless otherwise noted, the long-term redox processes were performed for up to 4000 steps using a coated ITO electrode by stepping a double potential between 0.0 and +1.5 V for the Fe(II)- and Ru(II)-MEPEs, and between −0.5 and +1.0 V for the Co(II)-based series. All the experiments were carried out in an argon-saturated acetonitrile solution of n-Bu_4NClO_4 (0.1 M) using a platinum wire as counter electrode, and Ag/AgCl as reference electrode. [b] Percent loss after 36 steps. [c] After 2000 steps. [d] After 600 steps. [e] After 300 steps. [f] Cannot be determined because of the weak $d-d^*$ transitions.

To inspect the effect of oxygen on the electrochromic property, multiple redox switching experiments were performed on several selected MEPEs in an oxygen-saturated acetonitrile solution of n-Bu_4NClO_4 (0.1 M). The results show that the loss of optical intensity is increased only slightly after 4000 double-potential cycles under oxygen. As a typical example, 25 vs 22% of the optical intensity is lost for **RuL4-MEPE** in the presence or absence of oxygen. The stability was also inspected by a long-term standing of the MEPE solutions at ambient environment; no changes are observed after longer than 6 months (Figure S3). These results indicate that the materials are highly stable under various applied conditions.

Our investigation reveals that the unsubstituted MEPEs are slightly less stable than the OMe-functionalized analogues as a comparison of **RuL1-MEPE** vs **RuL3-MEPE** and **RuL2-MEPE** vs **RuL4-MEPE** shows, although the Fe(II)-based unsubstituted MEPEs display an equally good stability as the OMe-functionalized analogues. In sharp contrast to the MEPEs with OMe-modified and unsubstituted ligands, MEPEs with the electron-withdrawing Br-substituted ligands, **FeL5-MEPE** and **RuL5-MEPE**, are unstable with an absorbance loss of approximately 50% within only 600 cycles.

Thus, the stability of MEPEs is mainly ligand-dependent, which can be rationalized on the basis of the electronic nature of the substituents at the peripheral pyridines. Apparently, the interactions between the ligands and metal ions are strengthened by electron-rich OMe groups and, consequently, lead to a high resistance against fatigue of the resulting MEPEs. In contrast, an electron-deficient substituent weakens the coordination between the ligands and metal ions, thereby inducing deterioration during the redox processes.

The stability of the Co(II)-MEPEs is probed by monitoring the changes of the $d-d^*$ transition as a function of time. Although the OMe- and Br-substituted materials (**CoL3-MEPE**−**CoL5-MEPE**) are not examined owing to their weak absorbance, the unsubstituted MEPEs, **CoL1-MEPE** and **CoL2-MEPE**, display good stability, showing a loss in absorbance of the $d-d^*$ transition within 2% after 300 steps.

Response Times. The response times of the MEPEs are examined by stepping the potentials between 0.0 and +1.5 V for the Fe(II)- and Ru(II)-MEPEs, and between −0.5 and +1.0 V for the Co(II)-MEPEs. For a comparison, MEPE films are

Table 4. Response Times of Fe(II)- and Ru(II)-MEPEs[a]

MEPEs	T_b (s)	T_c (s)	MEPEs	T_b (s)	T_c (s)
FeL1-MEPE[b]	2.12	2.06	**RuL1-MEPE**	2.25	1.41
FeL2-MEPE	2.08	2.02	**RuL2-MEPE**	2.58	1.44
FeL3-MEPE	0.65	0.69	**RuL3-MEPE**	1.01	1.17
FeL4-MEPE	0.89	0.96	**RuL4-MEPE**	0.99	1.01
FeL5-MEPE	>30	>30	**RuL5-MEPE**	2.97[c]	1.36

[a] Unless otherwise noted, response times for bleaching (T_b) and coloration (T_c) are given as an average of 150 redox cycles at applied potentials of +1.5 and 0.0 V. [b] Data for Fe(II)-based MEPEs taken from ref 21. [c] Because of the quick loss of optical intensity, response times are given as an average of 25 redox cycles.

prepared by casting equimolar amounts of material on an ITO slide with an area of ca. 8 mm × 25 mm, except for **FeL5-MEPE** (4.0 equiv) and **Co(II)-MEPEs** (6.0 equiv), where a larger amount is used because of the weak ϵ_{max}. The response times for **CoL3-MEPE**−**CoL5-MEPE** could not be determined reliably because of the weak $d-d^*$ transitions.

We note that MEPEs assembled from Co(II) exhibit a slow response time longer than 3 min under the applied conditions. The response times of Fe(II)- and Ru(II)-MEPEs are listed in Table 4. As a general observation, the unsubstituted MEPEs (**FeL1-MEPE** and **FeL2-MEPE**, and **RuL1-MEPE** and **RuL2-MEPE**) show response times of more than 2 s in most cases. Interestingly, this time is reduced to about 1 s or less in the assemblies whose ligands are modified by electron-donating OMe groups as exhibited by **FeL3-MEPE** and **FeL4-MEPE**, and **RuL3-MEPE** and **RuL4-MEPE**. On the contrary, substitution with the electron-withdrawing Br groups leads to prolonged response times in **FeL5-MEPE** and **RuL5-MEPE**, although the coloration time (T_c) of **RuL5-MEPE** is less affected. More interestingly, comparison of the bleaching (T_b) and coloration times (T_c) of each MEPE, especially the Ru(II)-based analogues, reveals that the bleaching process is relatively slower than the coloration process ($T_b > T_c$) for the unsubstituted MEPEs. This difference is further enlarged by attaching an electron-deficient Br group (**RuL5-MEPE**). However, incorporation of OMe groups into the ligands results in not only a reduced response time but also almost identical bleaching and coloration times. At this point, no definite mechanism can be proposed to explain this adequately because the charge transport kinetic, which governs the response times, is affected by several factors such as electron and ion mobility in the film. But one of the factors, here the electronic nature of the substituents, should be considered. The electron-donating or -withdrawing substituents may change the charge density in the polymer backbone, ultimately affecting the electron-transfer rates as well as the interaction strength of ligand and metal ion of both the oxidized (M^{3+}) and reduced (M^{2+}) states. On the other hand, the structure of the ligands may also affect the morphology of the films, thereby changing the diffusion of ions and the response times.[3]

Electrochromic Memory. Memory time (defined here as the ability of an ECM to remain transparent with the potential turned off) is also an important parameter if particular applications such as e-paper or displays are under consideration, but has not been investigated concerning the metallosupramolecular polymers. Our investigation shows that, for Fe(II)- and Ru(II)-MEPEs, the unsubstituted assemblies recover the colored state quite fast within a time scale of shorter than 30 s (Figure 8, inset). In sharp contrast, MEPEs functionalized either by electron-donating

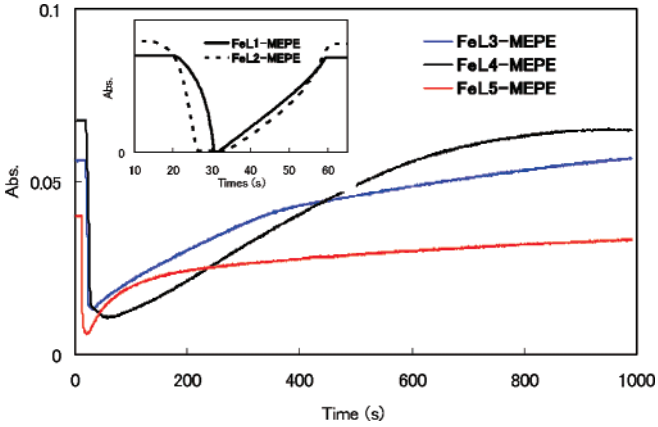

Figure 8. Optical memory times for **FeL3-MEPE**−**FeL5-MEPE**. Inset: **FeL1-MEPE** and **FeL2-MEPE** determined at λ_{max} of the MLCT band. For comparison, equal amounts of MEPEs (0.25 mM × 25 μL in MeOH) are coated on the ITO slides (8 × 30 mm^2). The experiments are carried out in an argon-saturated acetonitrile solution of n-Bu_4NClO_4 (0.1 M) using a platinum wire as counter electrode, and Ag/AgCl as reference electrode.

OMe or by electron-withdrawing Br groups show an enhanced memory time of up to 15 min for the **FeL3-MEPE**−**FeL5-MEPE**, and 8 min for the **RuL3-MEPE**−**RuL5-MEPE**. We propose that, through steric effects, the substituents (OMe or Br) at the 6-position of pyridine ring protect the metal center from being reduced by chemical reductants from the environment. The relatively shorter memory time exhibited by Ru(II)-MEPEs is mainly attributed to the higher redox potential of Ru(II)/(III) compared to Fe(II)/(III) couple (Table 2).[31] The optical memory effect is further controlled through the device design (e.g., carefully encapsulating the coating).

Conclusions

To search new electrochromic materials as well as to investigate the structure−property relationships of metal−ligand directed coordination complexes, three types of MEPEs (as differentiated by different metal ions) were assembled from various newly synthesized bisterpyridines and investigated in terms of their electrochromic properties. The presented MEPEs are soluble in a broad range of organic solvents and water. A key feature of these materials is that the colors are readily modified, covering the whole visible region through the design of the ligands or the choice of the metal ions, demonstrating the ease for color tuning, which is a topic of great concern in electrochromic applications. Study of electrochromic property reveals that introduction of the electron-donating OMe substituent to the ligand enhances markedly the switching stability and reversibility of the resulting MEPEs with an observed absorption loss of ca. 20% after 4000 double-redox steps. This substituent also reduces the switching potential of the derived MEPEs. The other properties such as the color, the response times, and the optical memory can be tuned either by the proper design of ligands or by the choice of metal centers. As such, the electrochromic MEPE materials described here have a high potential for technological applications for a broad range of purposes. Equally or even more importantly, the basic structure−property relationships established through this systematic study

(31) Storrier, G. D.; Colbran, S. B.; Craig, D. C. *J. Chem. Soc., Dalton Trans.* **1997**, 3011.

should lay the groundwork to serve for the de novo design of new ligands for new functional materials.

Experimental Section

Coated ITO electrodes for amperometric experiments were prepared by casting MEPE solutions in MeOH (or 4:1 MeOH/H_2O for Ru(II)-MEPEs) on an ITO slide with an area of ca. 25 mm × 8 mm, followed by slowly evaporating the solvent and drying at 50 °C for 10 min (70 °C for Ru(II)-based MEPEs). The amount of MEPEs is ca. 6.3 μmol for **FeL1-MEPE**−**FeL4-MEPE** and Ru(II)-MEPEs, 37.5 μmol for Co(II)-MEPEs, and 25 μmol for **FeL4-MEPE**.

Acknowledgment. We thank the Ministry of Education, Culture, Sports, Sciences, and Technology, Japan, for financial support.

Supporting Information Available: Detailed synthetic procedures and characterization for ligands and MEPEs, methods for optical, electrochemical, and electrochromic analyses, and X-ray crystallographic information. This material is available free of charge via the Internet at http://pubs.acs.org.

JA710380A